Inorg. Chem. **2006**, *45*, 6694–6705

Coordination Polymers with End-On Azido and Pyridine Carboxylate *N*-Oxide Bridges Displaying Long-Range Magnetic Ordering with Low Dimensional Character

Zheng He, Zhe-Ming Wang,* Song Gao, and Chun-Hua Yan*

Beijing National Laboratory for Molecular Sciences, State Key Lab of Rare Earth Materials Chemistry and Applications and PKU−HKU Joint Lab on Rare Earth Materials and Bioinorganic Chemistry, Peking University, Beijing 100871, China

Received February 9, 2006

A series of 2D and one 3D transition-metal–azido coordination polymers with pyridine carboxylate *N*-oxide, isonicotinate *N*-oxide (INO), and nicotinate *N*-oxide (NNO) as the coligands were synthesized by a hydrothermal method and structurally and magnetically characterized. These complexes have the formulas $[M(L)(N_3)(H_2O)]_n$ (L = INO and M = Mn, **1·Mn**; Co, **2·Co**; Ni, **3·Ni** and L = NNO and M = Mn, **4·Mn**; Co, **5·Co**; Ni, **6·Ni**) and $[Cu(L)(N_3)(H_2O)_{0.5}]_n$ (L = INO, **7·Cu**; NNO, **8·Cu**). All complexes consist of end-on azido and syn-syn carboxylato mixed-bridged M–N_3/COO chains that are further linked by the pyridine *N*-oxide group of the INO or NNO to give rise to 2D layered structures for **1·Mn**, **2·Co**, **3·Ni**, **4·Mn**, **5·Co**, **6·Ni**, and **8·Cu** and a 3D framework for **7·Cu**. The high-temperature magnetic susceptibilities are dominated by low-dimensional behavior while long-range ordering sets in at low temperatures. The Mn complexes are antiferromagnets, and the others are metamagnets. In addition, **5·Co** exhibits slow magnetic relaxation behavior at low temperatures. The metamagnetism in each case is due to strong intrachain ferromagnetic interactions and weak interchain antiferromagnetic ones.

Introduction

In the past two decades, the field of molecular magnetic materials has been experiencing much success in creating a number of new magnets.[1] Especially, the developments of low-dimensional magnets, for example, single-molecule-magnets (0D),[2] single-chain-magnets (1D, SCM),[3] and others showing low-dimensional magnetic features (1D or 2D) such as metamagnetism,[4] bridge the gap between paramagnetism and 3D long-range magnetic ordering and cover a wide range of spin dynamics. Coordination chemistry provides an effective approach to design and prepare these low-dimensional magnetic systems when magnetic transition-metal ions are assembled into coordination polymers by employing suitable ligands, both short bridging ones mediating effectively near-neighbor magnetic interactions and the auxiliary ones or coligands tuning the final structures as well as the secondary magnetic interactions in the materials.

Among the most used short bridging ligands such as cyanide, dicyanamide,[5] oxalate,[6] and azide (N_3^-), the latter has proved to be very versatile by displaying remarkable diversities in both crystal engineering and magnetism.[7] This

* To whom correspondence should be addressed. Tel. 86-10-6275-4179. Fax: +86-10-6275-4179. E-mail: yan@pku.edu.cn (C.-H.Y.), zmw@pku.edu.cn (Z.-M.W.).

(1) (a) Kahn, O. *Adv. Inorg. Chem.* **1995**, *43*, 179. (b) See the Proceedings of the International Conference of Molecule-Based Magnets. *Polyhedron* **2003**, *22*, 1725; **2005**, *24*, 2063.

(2) See, for example, (a) Ritter, S. K. *Chem. Eng. News* **2004**, *82*, 29. (b) Gatteschi, D.; Sessoli, R. *Angew. Chem., Int. Ed.* **2003**, *42*, 268. (c) Wernsdorfer, W.; Aliaga-Alcalde, N.; Hendrickson, D. N.; Christou, G. *Nature* **2002**, *416*, 406.

(3) See, for example, (a) Caneschi, A.; Gatteschi, D.; Lalioti, N.; Sangregorio, C.; Sessoli, R.; Venturi, G.; Vindigni, A.; Rettori, A.; Pini, M. G.; Novak, M. A. *Angew. Chem., Int. Ed.* **2001**, *40*, 1760. (b) Clérac, R.; Miyasaka, H.; Yamashita, M.; Coulon, C. *J. Am. Chem. Soc.* **2002**, *124*, 12837. (c) Lescouëzec, R.; Vaissermann, J.; Ruiz-Pérez, C.; Lloret, F.; Carrasco, R.; Julve, M.; Verdaguer, M.; Dromzee, Y.; Gatteschi, D.; Wernsdorfer, W. *Angew. Chem., Int. Ed.* **2003**, *42*, 1483.

(4) (a) Pereira, C. L. M.; Pedroso, E. F.; Stumpf, H. O.; Novak, M. A.; Ricard, L.; Ruiz-García, R.; Rivière, E.; Journaux, Y. *Angew. Chem., Int. Ed.* **2004**, *43*, 955. (b) Zeng, M.-H.; Zhang, W.-X.; Sun, X.-Z.; Chen, X.-M. *Angew. Chem., Int. Ed.* **2005**, *44*, 3079. (c) Matsumoto, N.; Sunatsuki, Y.; Miyasaka, H.; Hashimoto, Y.; Luneau, D.; Tuchagues, J.-P. *Angew. Chem., Int. Ed.* **1999**, *38*, 171.

(5) Jensen, P.; Price, D. J.; Batten, S. R.; Moubaraki, B.; Murray, K. S. *Chem.—Eur. J.* **2000**, *6*, 3186 and references therein.

(6) Decurtins, S.; Pellaux, R.; Antorrena, G.; Palacio, F. *Coord. Chem. Rev.* **1999**, *192*, 841.

(7) Ribas, J.; Escuer, A.; Monfort, M.; Vicente, R.; Cortés, R.; Lezama, L.; Rojo, T. *Coord. Chem. Rev.* **1999**, *193−195*, 1027.

10.1021/ic060225w CCC: $33.50
Published on Web 07/26/2006

particular property is due to the fact that azide can link metal ions in μ-1,1 (end-on, EO); μ-1,3 (end-to-end, EE); μ-1,1,3; or other modes, resulting in numerous materials of low dimensionalities (chains[3d,8,9] or layers[10]). The magnetic exchange mediated via an azido bridge can be ferro- or antiferromagnetic, depending on the bridging mode and bonding parameters. It has been widely stated that the exchange is generally ferromagnetic in nature for the EO mode and antiferromagnetic for the EE mode, although an increasing number of exceptions have been reported recently.[7,11]

The structures and thus the magnetic properties of metal−azido systems are obviously sensitive to the coligands employed. To date, various coligands have been introduced into the metal−azido system, giving rise to an abundant range of compounds, namely, from discrete molecular species (0D) to 1D, 2D, and 3D polymeric complexes showing a wide variety of magnetic properties. For example, the employment of monodentate pyridyl derivatives R-pyridine with the R group attached generally in the meta or para position[8,10a,b] and multidentate chelating N-donor ligands[9,10c] that block part of the coordination sites of the metal ions has led to a series of 1D and 2D compounds with general formulas $[M(L)_2(N_3)_2]_n$ and $[M(L)(N_3)_2]_n$, which exhibit ferrimagnetism, spin canting, and SCM. On the other hand, divergent rigid bridging ligands, such as pyrazine and 4,4′-bipyridine, are used to connect the parallel $M-N_3$ chains or layers to generate 2D or 3D network structures, and they display ferromagnetic and metamagnetic behaviors.[10d−f]

In this study, two isomers of pyridine carboxylate *N*-oxide, isonicotinate *N*-oxide (INO), and nicotinate *N*-oxide (NNO), are chosen as the coligands for incorporation into the metal−azido system. The choice of these two ligands is based on several considerations: (i) The carboxylato group in INO or NNO may bind to metal ions with various coordination modes, allowing for varied magnetic interactions.[12] (ii) The carboxylato group may coexist with the azido ion to bridge adjacent metal centers, giving rise to mixed-bridged complexes. Although a few complexes containing mixed azido and carboxylato bridges have hitherto been reported,[13] and some attention has been devoted to explain the unique magnetic properties of such mixed-bridged Cu^{2+} complexes,[13b,c] little attention has been devoted to the investigation of other azido and carboxylato mixed-bridged metal complexes except Cu^{2+} complexes. Thus, a study of complexes with two dissimilar bridges may provide useful information on magnetostructural correlation. (iii) Both the carboxylato and the *N*-oxide groups of INO and NNO have the ability to coordinate metal ions, which makes INO and NNO good linkers to connect metal−azido skeletons into coordination networks of high dimensionality. However, as the ligands are long spacers, they will magnetically separate the magnetic metal−azido skeletons and thus result in low-dimensional magnetic behaviors. (iv) The different coordination geometries exhibited by INO and NNO ligands may have influence on the structures of the outcome frameworks, as observed in our previous work,[14] as well as the magnetism of the materials. Here, we report the hydrothermal synthesis, crystal structures, and magnetic properties of a series of 2D and one 3D transition-metal−azido coordination polymers with INO and NNO as coligands. The general formulas of the complexes are $[M(L)(N_3)(H_2O)]_n$ (L = INO and M = Mn, **1·Mn**; Co, **2·Co**; Ni, **3·Ni** and L = NNO and M = Mn, **4·Mn**; Co, **5·Co**; Ni, **6·Ni**) and $[Cu(L)(N_3)(H_2O)_{0.5}]_n$ (L = INO, **7·Cu**; NNO, **8·Cu**). All complexes consist of mixed EO azido and syn-syn carboxylato-bridged $M-N_3$/COO chains that are further linked by the pyridine *N*-oxide of INO or NNO to give rise to 2D coordination layer structures of **1·Mn**, **2·Co**, **3·Ni**, **4·Mn**, **5·Co**, **6·Ni**, and **8·Cu** and a 3D coordination framework of **7·Cu**. The magnetic properties reveal low-dimensional behaviors at high temperatures and long-range ordering at lower temperatures.

Experimental Section

Materials and Apparatus. All starting chemicals were commercially available reagents of analytical grade and were used without further purification. Elemental analyses (C, H, and N) were performed on an Elementar Vario EL analyzer. IR spectra were recorded on a Nicolet Magna-IR 750 spectrometer equipped with a Nic-Plan microscope. DC magnetic data of compounds **1·Mn**−**8·Cu** were obtained on a Quantum Design MPMS-XL5 SQUID system, and zero-field AC magnetic susceptibility data for **2·Co** and **5·Co** were obtained on an Oxford Maglab2000 system. The

(8) (a) Escuer, A.; Vicente, R.; El Fallah, M. S.; Goher, M. A. S.; Mautner, F. A. *Inorg. Chem.* **1998**, *37*, 4466. (b) Abu-Youssef, M. A. M.; Escuer, A.; Gatteschi, D.; Goher, M. A. S.; Mautner, F. A.; Vicente, R. *Inorg. Chem.* **1999**, *38*, 5716. (c) Abu-Youssef, M. A. M.; Escuer, A.; Goher, M. A. S.; Mautner, F. A.; Reib, G.; Vicente, R. *Angew. Chem., Int. Ed.* **2000**, *39*, 1624. (d) Hong, C. S.; Koo, J.-e.; Son, S.-K.; Lee, Y. S.; Kim, Y.-S.; Do, Y. *Chem.−Eur. J.* **2001**, *7*, 4243.

(9) (a) Viau, G.; Lombardi, M. G.; Munno, G. D.; Julve, M.; Lloret, F.; Faus, J.; Caneschi, A.; Clemente-Juan, J. M. *Chem. Commun.* **1997**, 1195. (b) Mukherjee, P. S.; Dalai, S.; Zangrando, E.; Lloretc, F.; Chaudhuri, N. R. *Chem. Commun.* **2001**, 1444. (c) Monfort, M.; Resino, I.; Fallah, M. S. E.; Ribas, J.; Solans, X.; Font-Bardia, M.; Stoeckli-Evans, H. *Chem.−Eur. J.* **2001**, *7*, 280. (d) Gao, E.-Q.; Bai, S.-Q.; Wang, C.-F.; Yue, Y.-F.; Yan, C.-H. *Inorg. Chem.* **2003**, *42*, 8456.

(10) (a) Escuer, A.; Cano, J.; Goher, M. A. S.; Journaux, Y.; Lloret, F.; Mautner, F. A.; Vicente, R. *Inorg. Chem.* **2000**, *39*, 4688. (b) Escuer, A.; Mautner, F. A.; Goher, M. A. S.; Abu-Youssef, M. A. M.; Vicente, R. *Chem. Commun.* **2005**, 605. (c) Gao, E.-Q.; Yue, Y.-F.; Bai, S.-Q.; He, Z.; Zhang, S.-W.; Yan, C.-H. *Chem. Mater.* **2004**, *16*, 1590. (d) Manson, J. L.; Arif, A. M.; Miller, J. S. *Chem. Commun.* **1999**, 1479. (e) Martín, S.; Barandika, M. G.; Lezama, L.; Pizarro, J. L.; Serna, Z. E.; de Larramendi, J. I. R.; Arriortua, M. I.; Rojo, T.; Cortés, R. *Inorg. Chem.* **2001**, *40*, 4109. (f) Fu, A.-H.; Huang, X.-Y.; Li, J.; Yuen, T.; Lin, C. L. *Chem.−Eur. J.* **2002**, *8*, 2239.

(11) Goher, M. A. S.; Cano, J.; Journaux, Y.; Abu-Youssef, M. A. M.; Mautner, F. A.; Escuer, A.; Vicente, R. *Chem.−Eur. J.* **2000**, *6*, 778 and references therein.

(12) (a) Rettig, S. J.; Thompson, R. C.; Trotter, J.; Xia, S.-H. *Inorg. Chem.* **1999**, *38*, 1360 and references therein. (b) Ruiz-Pérez, C.; Sanchiz, J.; Molina, M. H.; Lloret, F.; Julve, M. *Inorg. Chem.* **2000**, *39*, 1363. (c) Konar, S.; Mukherjee, P. S.; Drew, M. G. B.; Ribas, J.; Chaudhuri, N. R. *Inorg. Chem.* **2003**, *42*, 2545. (d) Rao, C. N. R.; Natarajan, S.; Vaidhyanathan, R. *Angew. Chem., Int. Ed.* **2004**, *43*, 1466.

(13) (a) Chow, M.-Y.; Zhou, Z.-Y.; Mak, T. C. W. *Inorg. Chem.* **1992**, *31*, 4900. (b) Escuer, A.; Vicente, R.; Mautner, F. A.; Goher, M. A. S. *Inorg. Chem.* **1997**, *36*, 1233. (c) Thompson, L. K.; Tandon, S. S.; Lloret, F.; Cano, J.; Julve, M. *Inorg. Chem.* **1997**, *36*, 3301. (d) Chen, H.-J.; Mao, Z.-W.; Gao, S.; Chen, X.-M. *Chem. Commun.* **2001**, 2320. (e) Mialane, P.; Dolbecq, A.; Rivière, E.; Marrot, J.; Sécheresse, F. *Angew. Chem., Int. Ed.* **2004**, *43*, 2274. (f) Liu, F.-C.; Zeng, Y.-F.; Li, J.-R.; Bu, X.-H.; Zhang, H.-J.; Ribas, J. *Inorg. Chem.* **2005**, *44*, 7298.

(14) He, Z.; Wang, Z.-M.; Yan, C.-H. *CrystEngComm.* **2005**, *7*, 143.

experimental susceptibilities were corrected for the diamagnetism of the constituent atoms (-1.07×10^{-4}, -1.05×10^{-4}, -1.03×10^{-4}, and -1.04×10^{-4} emu mol^{-1} for Mn, Co, Ni, and Cu compounds, respectively)[15] and the experimentally measured background of the sample holders. Specific heat data between 2 and 20 K were obtained on a Quantum Design PPMS-6000 system, under zero and 1000 Oe fields.

Synthesis. All compounds were prepared by hydrothermal reaction. Typically for **1·Mn**, a mixture of HINO (72 mg, 0.50 mmol), $MnCl_2 \cdot 4H_2O$ (99 mg, 0.50 mmol), NaN_3 (131 mg, 1.0 mmol), and H_2O (3.0 mL) was sealed in a Teflon-lined stainless steel vessel (25 mL), heated at 150 °C for 3 days under autogenous pressure, and then cooled to room temperature. Yellow block crystals of **1·Mn** were harvested in a yield of 48% based on Mn. Similar procedures employing other metal salts and HINO or HNNO produced crystals of **2·Co**−**8·Cu** in yields of 40−81%. For **3·Ni** and **6·Ni**, it was proved, after several attempts of adjusting the synthesis conditions, that crystals suitable for single-crystal X-ray diffraction were difficult to obtain, but microcrystals of the pure phase were formed. Anal. Calcd for **1·Mn**, $C_6H_6MnN_4O_4$: C, 28.48; H, 2.39; N, 22.14. Found: C, 28.38; H, 2.44; N, 22.15. IR bands (cm^{-1}): 3342w, 3117w, 3060w, 2068vs, 1604s, 1553m, 1397s, 1213m, 1178w, 1145w, 878w, 863w, 785w, 683w. Anal. Calcd for **2·Co**, $C_6H_6CoN_4O_4$: C, 28.03; H, 2.35; N, 21.79. Found: C, 28.00; H, 2.36; N, 21.95. IR bands (cm^{-1}): 3345w, 3121w, 3060w, 2067vs, 1600s, 1555m, 1392s, 1302w, 1200m, 1179w, 1144w, 878w, 864w, 784w, 685w. Anal. Calcd for **3·Ni**, $C_6H_6NiN_4O_4$: C, 28.06; H, 2.35; N, 21.81. Found: C, 27.67; H, 2.46; N, 21.51. IR bands (cm^{-1}): 3352m, 3123m, 3059w, 2071vs, 1613vs, 1556s, 1394s, 1309w, 1200m, 1179m, 1144m, 879w, 864m, 786w, 685w. Anal. Calcd for **4·Mn**, $C_6H_6MnN_4O_4$: C, 28.48; H, 2.39; N, 22.14. Found: C, 28.44; H, 2.47; N, 22.24. IR bands (cm^{-1}): 3488w, 3454m, 3124w, 2077vs, 1672w, 1624s, 1597s, 1572s, 1432w, 1405s, 1227m, 1221m, 1130w, 945w, 801m, 770m, 688w, 662w. Anal. Calcd for **5·Co**, $C_6H_6CoN_4O_4$: C, 28.03; H, 2.35; N, 21.79. Found: C, 28.07; H, 2.50; N, 21.80. IR bands (cm^{-1}): 3498m, 3455m, 3359m, 3131m, 3122m, 2068vs, 1675m, 1627s, 1598s, 1574vs, 1433m, 1403s, 1225m, 1216m, 1130w, 943w, 803m, 770m, 689w, 664w. Anal. Calcd for **6·Ni**, $C_6H_6NiN_4O_4$: C, 28.06; H, 2.35; N, 21.81. Found: C, 27.95; H, 2.50; N, 21.86. IR bands (cm^{-1}): 3519w, 3473w, 3155w, 3121w, 2089m, 2068vs, 1678w, 1622s, 1600s, 1575s, 1433w, 1406s, 1226m, 1217w, 1131w, 945w, 803w, 770w, 692w, 666w. Anal. Calcd for **7·Cu**, $C_6H_5CuN_4O_{3.5}$: C, 28.52; H, 1.99; N, 22.17. Found: C, 28.30; H, 2.20; N, 22.51. IR bands (cm^{-1}): 3636vw, 3463vw, 3341vw, 3116vw, 2082vs, 1619m, 1587s, 1552m, 1405vs, 1274w, 1234m, 1190w, 1152w, 868w, 779w, 682w. Anal. Calcd for **8·Cu**, $C_6H_5CuN_4O_{3.5}$: C, 28.52; H, 1.99; N, 22.17. Found: C, 28.65; H, 2.19; N, 22.46. IR bands (cm^{-1}): 3553vw, 3344vw, 3126vw, 3090w, 2087vs, 1615m, 1585s, 1563s, 1407s, 1279m, 1228m, 1123w, 1021w, 950w, 807m, 762m, 669w.

***CAUTION**: Although not encountered in our experiments, azido compounds of metal ions are potentially explosive. Only a small amount of the materials should be prepared, and it should be handled with care.*

X-ray Crystallography. Diffraction intensity data for the single crystals of the Mn, Co, and Cu compounds were collected at room temperature on a Nonius Kappa CCD diffractometer equipped with graphite-monochromated Mo Kα radiation (λ = 0.710 73 Å).[16] Empirical absorption corrections were applied using the Sortav program.[17] All structures were solved by the direct method and refined by the full-matrix least-squares method on F^2 with anisotropic thermal parameters for all non-hydrogen atoms.[18] Hydrogen atoms of the coordinated water molecule for compounds **1·Mn**, **2·Co**, **4·Mn**, and **5·Co** and those of the solvent water molecule for compound **8·Cu** were added by difference Fourier mapping and refined isotropically with constraints for the ideal geometry of a water molecule with an O−H distance of 0.96 Å and a H−O−H angle of 105°. Other hydrogen atoms were added by calculation positions. Crystallographic data for the structures reported in this paper have been deposited with the Cambridge Crystallographic Data Centre as CCDC 291000−291005.

Powder X-ray diffraction (PXRD) patterns for samples of all compounds were obtained on a Rigaku D/max 2000 diffractometer at room temperature with Cu Kα radiation in a flat plate geometry.

Results and Discussion

Synthesis and IR Spectra. The series of compounds, $[M(INO)(N_3)(H_2O)]_n$ (M = Mn, **1·Mn**; Co, **2·Co**; Ni, **3·Ni**), $[M(NNO)(N_3)(H_2O)]_n$ (M = Mn, **4·Mn**; Co, **5·Co**; Ni, **6·Ni**), and $[Cu(L)(N_3)(H_2O)_{0.5}]_n$ (L = INO, **7·Cu**; NNO, **8·Cu**), with a M/L/N_3 ratio of 1:1:1 were obtained by the hydrothermal reaction of M^{2+}, HL, and NaN_3 in a 1:1:2 molar ratio. The excess amount of NaN_3 acts as a base to deprotonate the HL ligand. We have observed in our previous study[14] that the three isomers of pyridine carboxylate *N*-oxide, PNO (picotinate *N*-oxide), NNO, and INO, with different coordination geometries, would lead to different crystal structures. In this investigation, we also tried to employ the three isomers as the coligands in metal−azido system. We succeeded in getting compounds containing both NNO/INO and azido ligands; however, in the case of PNO, only mononuclear compounds of $[M(PNO)_2(H_2O)_2]$ without the azido anion were obtained. This may be due to the strong chelating ability of PNO that excludes the coordination of azide anions to metal ions. Because they are not magnetically interesting, we do not include them in this paper. We tried to obtain crystals of **3·Ni** and **6·Ni** suitable for single-crystal X-ray diffraction without success. However, the PXRD patterns of the resulting microcrystals of **3·Ni** and **6·Ni** agree well with the simulated ones based on the crystal structures of **1·Mn** and **2·Co** and those of **4·Mn** and **5·Co**, respectively, indicating that **3·Ni** is isomorphous with **1·Mn** and **2·Co** and **6·Ni** with **4·Mn** and **5·Co** (Figure S1, Supporting Information). Finally, the PXRD patterns of all of the compounds confirmed their phase purity, as shown in Figure S1 of the Supporting Information.

The IR spectra of the complexes (see the Experimental Section) display characteristic bands of the azido bridges and the carboxylato group. In the region expected for the $\nu_{as}(N_3)$ absorption, all of the compounds exhibit only one single

(15) Boudreaux, E. A.; Mulay, J. N. *Theory and Application of Molecular Diamagnetism*; J. Wiley and Sons: New York, 1976.

(16) (a) *Collect*; Nonius BV: Delft, The Netherlands, 1998. (b) *HKL2000*; *maXus*; University of Glasgow: Glasgow, Scotland, U. K.; Nonius BV: Delft, The Netherlands; MacScience Co. Ltd.: Yokohama, Japan, 2000.

(17) (a) Blessing, R. H. *Acta Crystallogr., Sect. A* **1995**, *51*, 33. (b) Blessing, R. H. *J. Appl. Crystallogr.* **1997**, *30*, 421.

(18) (a) Sheldrick, G. M. *SHELXTL*, version 5.1; Bruker Analytical X-ray Instruments Inc.: Madison, Wisconsin, 1998. (b) Sheldrick, G. M. *SHELX-97*, PC version; University of Göttingen: Göttingen, Germany, 1997.

Table 1. Crystallographic Data and Structure Refinement Results for **1·Mn**−**8·Cu**

compound	**1·Mn**	**2·Co**	**4·Mn**	**5·Co**	**7·Cu**	**8·Cu**
formula	$C_6H_6MnN_4O_4$	$C_6H_6CoN_4O_4$	$C_6H_6MnN_4O_4$	$C_6H_6CoN_4O_4$	$C_6H_5CuN_4O_{3.5}$	$C_6H_5CuN_4O_{3.5}$
fw	253.09	257.08	253.09	257.08	252.68	252.68
cryst syst	triclinic	triclinic	monoclinic	monoclinic	orthorhombic	monoclinic
space group, *Z*	$P\bar{1}$, 2	$P\bar{1}$, 2	$P2_1/c$, 8	$P2_1/c$, 8	*Pnma*, 4	*C*2/*c*, 8
a [Å]	6.5436(3)	6.5324(3)	11.1762(4)	11.1894(5)	16.7625(6)	16.3442(5)
b [Å]	7.7601(4)	7.4879(4)	7.7306(3)	7.5509(3)	6.4316(2)	6.9380(2)
c [Å]	9.2478(4)	9.1313(6)	20.1033(8)	20.008(1)	8.3070(3)	14.6374(6)
α [deg]	99.675(2)	100.167(3)	90	90	90	90
β [deg]	95.845(2)	95.164(4)	91.004(1)	92.380(2)	90	105.409(1)
γ [deg]	108.725(2)	107.418(3)	90	90	90	90
V [Å^3]	432.27(3)	414.60(4)	1736.6(1)	1689.03(13)	895.58(5)	1600.16(9)
ρ_{calcd} [g cm^{-3}]	1.944	2.059	1.936	2.022	1.874	2.106
μ [mm^{-1}]	1.527	2.070	1.521	2.032	2.432	2.722
$R_1{}^a$ [$I > 2\sigma(I)$]	0.0304	0.0328	0.0432	0.0370	0.0321	0.0290
$wR_2{}^b$ (all data)	0.0706	0.0637	0.0877	0.0727	0.1079	0.0683
GOF	0.936	0.897	0.842	0.863	0.994	0.914

^{a} $R_1 = \sum||F_o| - |F_c||/\sum|F_o|$. ^{b} $wR_2 = \{\sum[w(F_o^2 - F_c^2)^2]/\sum[w(F_o^2)^2]\}^{1/2}$.

Chart 1. M−N_3/COO Chain, with Bridges of One EO Azido and One syn-syn Carboxylate Linking Metal Ion, as the Basic Structure Motif in This Work

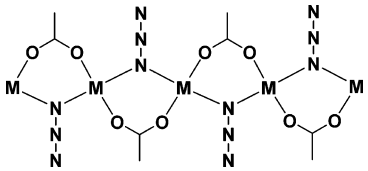

sharp and strong band at ca. 2070 cm^{-1}, attributable to the presence of only an EO azido bridge in the structures.[19] For complexes **1·Mn**, **2·Co**, and **3·Ni**, the two strong absorptions at ca. 1555 and 1392 cm^{-1} are assignable to the ν_{as}(COO) and ν_s(COO) modes of the L ligand, which occur at ca. 1600 and 1403 cm^{-1} for complexes **4·Mn**, **5·Co**, and **6·Ni** and 1587 and 1405 cm^{-1} for complexes **7·Cu** and **8·Cu**, respectively.[16] In addition, bands at ca. 3340 and 1600 cm^{-1} are assigned to the O−H stretching and bending of the coordination or solvent water in the structures.[20]

Crystal Structures. Detailed crystallographic data are summarized in Table 1. The selected molecular geometries are listed in Tables S1−S4 of the Supporting Information. The common structural feature of these compounds is the 1D M−N_3/COO chain composed of metal ions linked by one EO azido and one syn-syn carboxylato bridge simultaneously (Chart 1). To the best of our knowledge, this kind of linkage has rarely been observed before.[13] Around each metal ion, two EO azido ligands reside in trans positions, and the same is the case for the two oxygen atoms from two syn-syn carboxylato bridges. With the ligands, INO or NNO, providing the carboxylato bridges and additional coordinating *N*-oxide groups, the chains are connected into 2D coordination layers for **1·Mn**, **2·Co**, **3·Ni**, **4·Mn**, **5·Co**, **6·Ni**, and **8·Cu** and a 3D framework for **7·Cu**. From the viewpoint of magnetostructural relationship, the intrachain interactions are expected to be strong and the interchain ones weak. This difference of intra- and interchain interactions indeed results in interesting magnetic behaviors observed for these compounds (vide supra). More structural details concerning the specific compounds are given below.

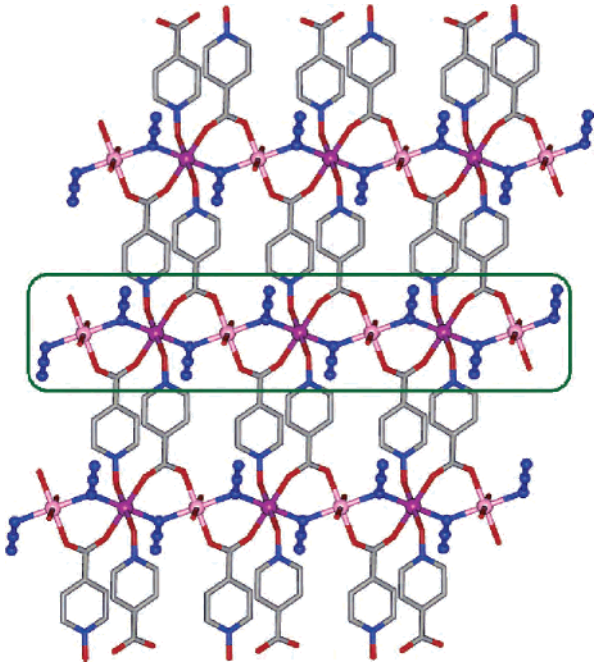

Figure 1. One layer in **2·Co** (highlighted in the box is the Co−N_3/COO chain; Co1 and Co2 are represented in purple and pink, respectively).

Structures of 1·Mn, 2·Co, and 3·Ni. Complexes **1·Mn**, **2·Co**, and **3·Ni** are isostructural (Table 1; Table S1 and Figure S1a of the Supporting Information) and the structure of **2·Co** is described in detail here. **2·Co** contains 2D layers made up of Co−N_3/COO chains connected by the INO ligands (Figure 1). There are two crystallographically independent Co^{2+} ions, Co1 and Co2 (Figure S2a, Supporting Information), each lying at an inversion center but possessing different octahedral geometries. Co1 has an elongated coordination octahedron, while Co2 has a compressed one. The equatorial plane of Co1 consists of two nitrogen atoms from two azide ions [Co−N = 2.105(2) Å] and two carboxylate oxygen atoms from two INO ligands [Co−O = 2.114(2) Å], while two *N*-oxide oxygen atoms from the other two INO ligands occupy the axial sites [Co−O = 2.154(2) Å]. Co2 is equatorially coordinated by two azide ions [Co−

(19) Tandon, S. S.; Thompson, L. K.; Manuel, M. E.; Bridson, J. N. *Inorg. Chem.* **1994**, *33*, 5555.
(20) Nakamoto, K. *Infrared and Raman Spectra of Inorganic and Coordination Compounds*; Wiley: New York, 1986.

N = 2.137(2) Å] and two water oxygen atoms [Co−O = 2.162(2) Å] and axially by two carboxylate oxygen atoms from two INO ligands [Co−O = 2.040(2) Å]. Both Co−O and Co−N bond distances lie in the range of values reported for Co-carboxylato[21] and Co-azido[3d,22] compounds. The cis N/O−Co−N/O angles range from 86.9 to 93.1°, while trans ones are the ideal 180°. The Co−N_3/COO chain (Figure 1, highlighted part), in which Co1 and Co2 atoms alternate, runs along the *b* direction. The intrachain Co···Co separation is 3.744 Å, and the EO azide bridging angle Co−N−Co is 123.9°, which falls out of the usually observed range of 100−107° of the M−N−M angle for M = Cu, Ni, and Mn[13b] and is also much larger than the 100.5−116.0° of the Co−N−Co angle in other Co EO azido systems.[3d,9a,22,23]

The INO ligands, with carboxylato groups bridging the cobalt ions in one chain, provide *N*-oxide groups coordinating to the Co1 atoms in the neighboring chains. Therefore, the Co−N_3/COO chains are connected through INO ligands to afford a 2D layer along the *bc* plane (Figure 1), the interchain Co···Co separations spanned by INO being 9.131 and 9.237 Å. The layers are stacked along the *a* axis, and between them there are several sets of H bonds (Figure S2b and Table S1, Supporting Information). In **2·Co**, the *N*-oxide oxygen atom forms an O4−H···O3E (symmetry code E: $-x + 1, -y + 1, -z + 2$) H bond with the coordinated water molecule, the O···O distance and the O−H···O angle being 2.877 Å and 151°, respectively. It has been well-documented that *N*-oxide can mediate H bonds effectively.[24] The coordinated water molecules are also involved in H bonds with the azido ions, and these are O4−H···N3F and O4−H···N4F (symmetry code F: $x + 1, y, z$) with O···N distances of 3.213 and 3.185 Å and O−H···N angles of 142 and 155°, respectively. Worthy of note is that all of the interlayer Co ions are linked by O−H···O/N H bonds. The shortest interlayer Co···Co contact, via one pair of the three-atom O−H···O (*N*-oxide) H-bond bridge and another pair of the short O−H···N (azide) H-bond bridge, is Co1···Co2 at 6.485 Å, which is an important feature to be related to the magnetism.

1·Mn has the same structure as **2·Co**; however, it shows some significant difference in molecular geometries. The longer Mn−N/O distances and larger Mn···Mn separations are in relation to the larger ionic radius of Mn^{2+} versus Co^{2+}.[25] Mn1 has three pairs of Mn−N/O distances of 2.164, 2.212, and 2.255 Å with almost the same increment of 0.05 Å from the short to the long ones, and Mn2 has a compressed octahedron as Co2 in **2·Co**. The structure of **3·Ni** should be very close to that of **2·Co** considering the similarity of the PXRD patterns (Figure S1a, Supporting Information) and the ionic radii of the Co^{2+} and Ni^{2+} ions.

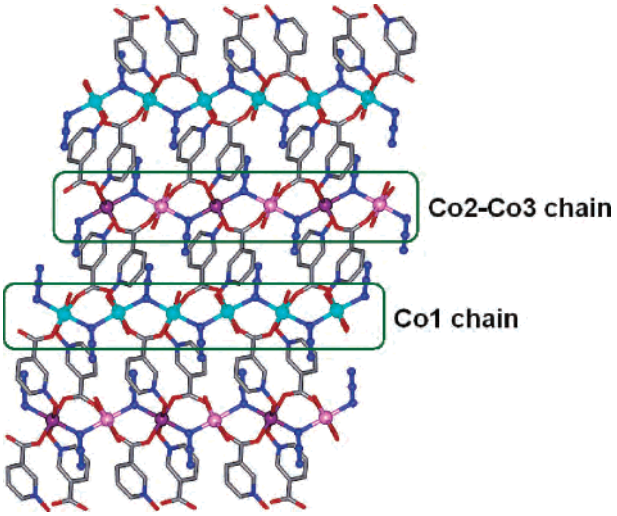

Figure 2. One layer in **5·Co** (highlighted in the boxes are the two kinds of Co−N_3/COO chains; Co1, Co2, and Co3 are represented in light blue, purple, and pink, respectively).

Structures of 4·Mn, 5·Co, and 6·Ni. The use of the NNO ligand instead of INO in the reaction system produced the three isomorphous complexes **4·Mn**, **5·Co**, and **6·Ni**, as confirmed by single-crystal structures (Table 1), PXRD patterns (Figure S1b, Supporting Information), elemental analysis, and IR spectra (Experimental Section). The structural similarity of **6·Ni** to **5·Co** was also proved by PXRD. The structure of **5·Co** is discussed as the representative. **5·Co** also consists of 2D layers in which Co−N_3/COO chains are connected through NNO ligands (Figure 2). Three unique Co^{2+} ions, Co1, Co2, and Co3, all possessing a distorted octahedral geometry, are found in the compound (Figure S3a, Supporting Information). However, unlike the Co^{2+} ions in **2·Co**, the Co−N/O distances for each Co^{2+} ion in **5·Co** show similar increments (Table S2, Supporting Information) from the short one to the long one; thus, the CoN_2O_4 octahedra possess no elongated or compressed patterns. Co1 is surrounded by one *N*-oxide oxygen atom from one NNO ligand, two carboxylate oxygen atoms from the other two NNO ligands, one water, and two nitrogen atoms from two azides [Co−N/O = 2.072(3) − 2.170(3) Å]. Both Co2 and Co3 atoms are located on inversion centers. For the Co2 atom, four oxygen atoms, two from *N*-oxide groups of two NNOs and two from carboxylato groups of the other two NNO ligands, and two nitrogen atoms from two azide ions make the coordination octahedron, with Co−N/O = 2.055(3)−2.172(3) Å. The environment of the Co3 atom consists of four oxygen atoms from two carboxylato groups of two NNO ligands, two waters, and two azido nitrogen atoms [Co−N/O = 2.092(3)−2.149(4) Å]. The Co−N/O distances are comparable with those in related compounds.[3d,21,22] The cis N/O−Co−N/O angles range from 81.7 to 99.4°, while the trans ones around Co1 range from 169.8 to 174.0°, and that around Co2/Co3 is the ideal 180°.

(21) (a) Kurmoo, M.; Estournès, C.; Oka, Y.; Kumagai, H.; Inoue, K. *Inorg. Chem.* **2005**, *44*, 217. (b) Sun, D.-F.; Ma, S.-Q.; Ke, Y.-X.; Petersen, T. M.; Zhou, H.-C. *Chem. Commun.* **2005**, 2663.
(22) (a) Papaefstathiou, G. S.; Escuer, A.; Raptopoulou, C. P.; Terzis, A.; Perlepes, S. P.; Vicente, R. *Eur. J. Inorg. Chem.* **2001**, 1567. (b) Wang, L.-Y.; Zhao, B.; Zhang, C.-X.; Liao, D.-Z.; Jiang, Z.-H.; Yan, S.-P. *Inorg. Chem.* **2003**, *42*, 5804.
(23) (a) Drew, M. G. B.; Esho, F. S.; Lavery, A.; Nelson, S. M. *J. Chem. Soc., Dalton Trans.* **1984**, 544. (b) Drew, M. G. B.; Harding, C. J.; Nelson, S. M. *Inorg. Chim. Acta* **1996**, *246*, 73. (c) Serna, Z. E.; Urtiaga, M. K.; Barandika, M. G.; Cortés, R.; Martin, S.; Lezama, L.; Arriortua, M. I.; Rojo, T. *Inorg. Chem.* **2001**, *40*, 4550.
(24) Sun, H.-L.; Gao, S.; Ma, B.-Q.; Batten, S. R. *CrystEngComm* **2004**, *6*, 579 and references cited therein.
(25) Cotton, F. A. *Advanced Inorganic Chemistry*; VCH: New York, 1999.

Two unique Co−N_3/COO chains are observed in **5·Co** (Figure 2, highlighted part). One consists of Co1 atoms only and the other of Co2 and Co3 atoms in a Co2−Co3−Co2−Co3 sequence, both running along the *b* direction. For the chain of Co1, the Co1···Co1 distance and Co1−N−Co1 angle are 3.782 Å and 122.1°, respectively, and for the chain of Co2 and Co3, the Co2···Co3 distance and the Co2−N−Co3 angle are 3.775 Å and 121.8°, respectively. The two types of chains are alternately interconnected through two kinds of NNO ligands. One has its *N*-oxide group coordinated to Co1 atoms of one chain of Co1, and its carboxylato group binds Co2 and Co3 atoms in the neighboring chain of Co2 and Co3 in the syn-syn mode. The other kind, which provides the syn-syn carboxylate group bridging Co1 atoms in one chain of Co1, coordinates to the Co2 atoms in the neighboring chain of Co2 and Co3 via its *N*-oxide group. The interchain Co···Co distances via NNO are 7.349−7.972 Å. Therefore, all NNO ligands link the two kinds of chains into a 2D layer parallel to the (1 0 −2) plane (Figure 2). The azide ions reside in the layer with their terminal nitrogen atoms involved in the intralayer O−H···N H bonds with the coordination water (Table S2, Supporting Information). These layers are held together through the weak C3−H···O6G (symmetry code G: $x, -y + {}^1/_2, z - {}^1/_2$) H bonds between the C−H group of the NNO ligands from one layer and the *N*-oxide oxygen from the neighboring ones, the C···O distance and the C−H···O angle being 3.216 Å and 124.7°, respectively (Figure S3b and Table S2, Supporting Information). These C−H···O H bonds interconnect Co atoms with the shortest interlayer Co···Co distance of 7.592 Å.

It is worth pointing out some detailed structural differences, mainly regarding the interchain interactions, between **2·Co** and **5·Co**, although they are both lamellar. These differences, which are related to the different magnetic behaviors of the two kinds of compounds discussed later, definitely result from the different coordination geometries of the bridging organic ligands, INO and NNO. Despite the minor difference in local molecular geometries (Tables S1 and S2, Supporting Information), the straight coordination geometry of INO affords a flat and thin layer structure in **2·Co**, and the azide ions slant out of the layer, involved in various H bonds between the neighboring layers; in particular, the shortest interlayer Co···Co separation is through three or four diamagnetic atoms via H bonds. Whereas in **5·Co**, the bent coordination geometry of NNO affords a more puckered and thicker layer. The azide ions only form H bonds within the layer, and through these H bonds, there are at least five diamagnetic atoms between the Co ions. The interlayer Co···Co separations are also separated by at least six diamagnetic atoms via the C−H···O H-bond bridges. All Co···Co linkages via the organic ligands, INO and NNO, have seven (for INO) or six (for NNO) diamagnetic atoms. Therefore, the interchain magnetic coupling in **2·Co** should be larger than that in **5·Co** considering the structural difference described above, similar to that for **1·Mn** versus **4·Mn** and **3·Ni** versus **6·Ni**.

Structure of 7·Cu. The structure of **7·Cu** is a 3D coordination framework consisting of Cu−N_3/COO chains

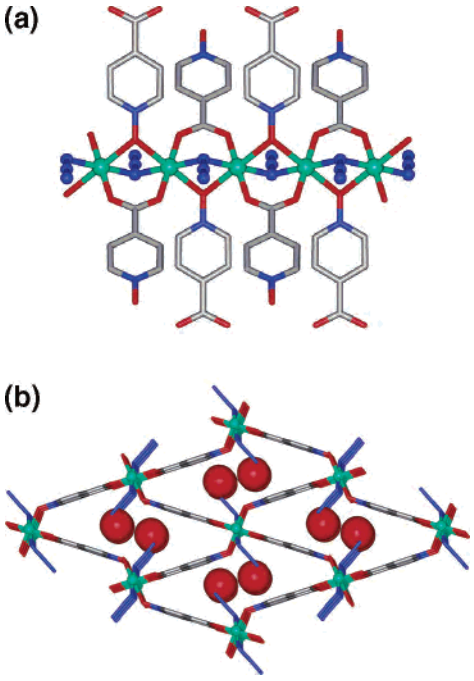

Figure 3. Structure of **7·Cu**: (a) the Cu−N_3/COO chain and (b) the three-dimensional network viewed along the *b* axis (the solvent water molecules are in the space-filling model, oxygen atoms only).

connected by INO ligands (Figure 3). The chains run along the *b* direction. The unique Cu^{2+} ion is located at an inversion center, and its coordination environment is an elongated octahedron (Figure S4 and Table S3, Supporting Information) in which the equatorial plane is made up of two carboxylate oxygen atoms from two INO ligands and two nitrogen atoms from two azides and the axial sites are occupied by two *N*-oxide oxygen atoms from the other two INO ligands. The equatorial Cu−N/O distances of 1.959(2) and 2.008(2) Å are substantially shorter than the axial Cu−O ones of 2.475(2) Å (Table S4, Supporting Information), and they match those observed in related compounds.[26] Besides the EO azido and the syn-syn carboxylato bridges, one μ_2-*N*-oxide group of the INO ligand links the adjacent copper centers additionally with long Cu−O distances (Figure 3a). From the magnetic point of view, the magnetic exchange interactions in the chains would be expected to depend predominantly on the bridges in the equatorial plane of Cu^{2+}, that is, the azido and carboxylato bridges. The *N*-oxide bridges with long axial Cu−O distances are considered to propagate negligible exchange or very weak antiferromagnetic exchange interaction.[27] The EO azido bridge connects two Cu centers with a Cu−N−Cu angle of 106.6° and a Cu···Cu separation of 3.216 Å.

(26) (a) Thompson, L. K.; Tandon, S. S.; Manuel, M. E. *Inorg. Chem.* **1995**, *34*, 2356. (b) Mukherjee, P. S.; Maji, T. K.; Mostafa, G.; Mallah, T.; Chaudhuri, N. R. *Inorg. Chem.* **2000**, *39*, 5147. (c) Graham, B.; Hearn, M. T. W.; Junk, P. C.; Kepert, C. M.; Mabbs, F. E.; Moubaraki, B.; Murray, K. S.; Spiccia, L. *Inorg. Chem.* **2001**, *40*, 1536.

(27) (a) Cortés, R.; Urtiaga, M. K.; Lezama, L.; Larramendi, J. I. R.; Arriortua, M. I.; Rojo, T. *J. Chem. Soc., Dalton Trans.* **1993**, 3685. (b) Commarmond, J.; Plumeré, P.; Lehn, J. M.; Agnus, Y.; Louis, R.; Weiss, R.; Kahn, O.; Morgenstern-Badarau, I. *J. Am. Chem. Soc.* **1982**, *104*, 6330. (c) Bkoeche-Waskman, I.; Sikorav, S.; Kahn, O. *J. Crystallogr. Spectrosc. Res.* **1983**, *13*, 303.

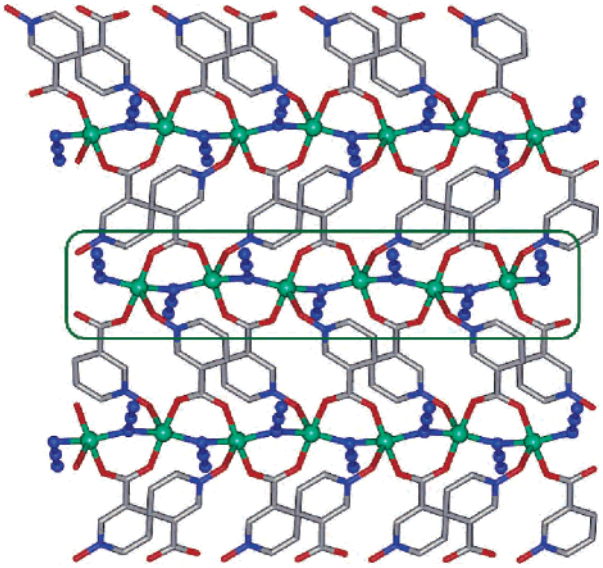

Figure 4. Layer in **8·Cu** (highlighted in the box is the Cu−N_3/COO chain).

The chains are further linked by INO ligands: the ligands with their carboxylato groups acting as bidentate syn-syn bridges in one chain are coordinated to pairs of Cu atoms in the adjacent chains via their *N*-oxide groups as monodentate μ_2 bridges and vice versa. Therefore, each INO ligand links four Cu atoms from two chains, and each Cu atom is coordinated by four INO ligands. Thus, each chain is connected to four neighboring ones through bridging INO ligands that radiate from the chain in different directions to generate a 3D structure (Figure 3b). The 3D coordination framework has rhombic channels of 9.35 × 9.35 Å (on the basis of Cu···Cu separations) along the *b* direction, and these channels are filled with solvent water and azido bridges that point outward from the chains. In addition, the solvent water molecules and the azide ions form O3−H···N3 and O3−H···N4 H bonds that further stabilize the structure, the O···N distances being 3.326 and 3.338 Å, respectively.

Structure of 8·Cu. Compound **8·Cu** is made up of 2D layers in which Cu−N_3/COO chains are interconnected through NNO ligands (Figure 4). The Cu^{2+} ion is five-coordinated in square-pyramidal geometry (Figure S5a, Supporting Information). Its basal plane consists of two carboxylate oxygen atoms from two NNOs with Cu−O distances of 1.964(2) and 1.959(2) Å and two azide nitrogen atoms with Cu−N distances of 1.986(2) and 1.998(2) Å, and the apical position is occupied by a *N*-oxide oxygen (O3) from the third NNO ligand with a longer Cu−O distance of 2.224(2) Å (Table S4, Supporting Information). The τ value of the coordination geometry of the Cu^{2+} ion defined by Addison et al.[28] is 0.22, confirming the distorted square-pyramidal geometry. The neighboring Cu^{2+} ions are doubly bridged by one EO azide and one syn-syn carboxylate of NNO, giving the Cu−N_3/COO chain along the *b* direction. Within the chain, the Cu···Cu separation is 3.522 Å, and the Cu−N−Cu angle is 124.3°, which is much larger than the values of 111.9 and 119.5° for known carboxylato/EO azido mixed-bridged copper chain compounds.[13b,c]

The NNO ligand, whose carboxylato group bridges one pair of Cu atoms in one chain, is bonded to one Cu atom in the neighboring chain via its *N*-oxide group. Therefore, the chains are linked by NNO ligands to give a 2D layer parallel to the *bc* plane (Figure 4). The layers are stacked along the *a* direction to form a 3D network with the interlayer space occupied by solvent water (Figure S5b, Supporting Information). Both the solvent water molecules and the azide ions that slant outward from the layers participate in C/O−H···O/N H bonds with the NNO ligands (Table S4, Supporting Information). Within the coordination layer, the shortest interchain Cu···Cu distance is 7.161 Å, while the interlayer one is 8.681 Å.

It is interesting to see again that the organic ligands, INO and NNO, direct the formation of different structures of **7·Cu** and **8·Cu**. Despite the similar Cu−N_3/COO chain, the differences lie not only in the local coordination geometry of the Cu^{2+} ion, the elongated octahedron in **7·Cu** versus the square pyramid in **8·Cu**, but also in the global coordination structures, the 3D framework of **7·Cu** versus the 2D lamellar one of **8·Cu**. The more divergent coordination geometry of INO versus that of NNO seems to contribute to this, as the ligands behaved in other systems.[14]

Magnetic Properties. As has been discussed above, the series of compounds are structurally featured as M−N_3/COO chains linked by INO or NNO ligands, as well as interchain H bonds. On the basis of the structures, it is reasonably expected that the intrachain magnetic coupling via the EO azido and the syn-syn carboxylato bridges is strong, while the interchain ones via ligands and H bonds are weak. Consequently, this series of compounds should have low-dimensional characteristics in its magnetism. Indeed, the two Mn compounds, **1·Mn** and **4·Mn**, are antiferromagnets with a low-dimensional feature; **5·Co** is basically a metamagnet but exhibits magnetic relaxation behavior at low temperatures, and the remaining five compounds are all metamagnets with strong intrachain ferromagnetic interactions and weak interchain antiferromagnetic ones. The basic magnetic data for all of the compounds are summarized in Table 2, and the details are discussed subsequently below.

1·Mn and 4·Mn. Both **1·Mn** and **4·Mn** are antiferromagnets. The temperature dependence of their susceptibilities under a 1 kOe applied field is shown in Figure 5. The experimental $\chi_M T$ values at 300 K are 4.11 and 4.13 emu mol^{-1} K for **1·Mn** and **4·Mn**, respectively, somewhat lower than the spin-only value (4.38 emu K mol^{-1} for $S = {}^5/_2$) expected for an uncoupled high-spin Mn(II) ion. Upon cooling, the $\chi_M T$ of both complexes decreases monotonically and tends to zero at low temperatures. The global feature indicates a dominant antiferromagnetic interaction in both compounds. The high-temperature magnetic susceptibility of both compounds obeys the Curie−Weiss law with $C = 4.97$ emu K mol^{-1} and $\theta = -36.8$ K for **1·Mn** and $C = 4.73$ emu K mol^{-1} and $\theta = -18.4$ K for **4·Mn**. The negative Weiss constants suggest intrachain antiferromagnetic coupling between Mn(II) ions. The Néel temperatures, T_N, of

(28) Addison, A. W.; Rao, T. N.; Reedjik, J.; van Rijn, J.; Verschoor, C. G. *J. Chem. Soc., Dalton Trans.* **1984**, 1349.

Table 2. Summary of Magnetic Properties of **1·Mn**−**8·Cu**

compd	C^a/emu mol^{-1} K	θ^b/K	$\chi_M T$ (300 K)/ emu mol^{-1} K	T_N/K	J^c/cm^{-1}	zJ'^d/cm^{-1}	g
1·Mn	4.97	−36.8	4.11	10.0	−2.49(3)	−0.92(5)	2.100(1)
2·Co	3.45	9.64	3.57	9.5	3.09(2)^e		2.702(1)^e
3·Ni	2.93	25.6	1.60	8.0	36(2)	−0.8(3)	2.24(1)
4·Mn	4.73	−18.4	4.13	8.5	−1.53(1)	−0.46(6)	2.062(1)
5·Co	3.64	6.89	3.73	5.3	2.06(2)^e		2.785(2)^e
6·Ni	1.47	27.3	1.62	6.0	26.1(7)	−0.6(2)	2.315(7)
7·Cu	0.58	28.7	0.64	2.5	80(4)	−0.17(2)	2.13(3)
8·Cu	0.53	32.3	0.57	3.5	48(1)	−0.84(2)	2.25(1)

[a] Curie constant. [b] Weiss constant. [c] Intrachain coupling. [d] Interchain coupling. [e] Above 40 K (see text).

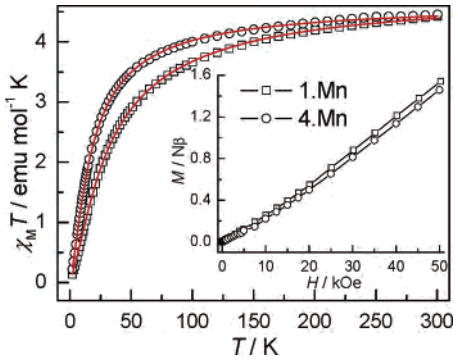

Figure 5. Plots of $\chi_M T$ vs T for **1·Mn** and **4·Mn** under an applied field of 1 kOe. Red solid lines represent the best theoretical fit. Inset: plot of M vs H for **1·Mn** (2 K) and **4·Mn** (1.8 K).

1·Mn and **4·Mn** were determined from the peak of d($\chi_M T$)/dT at 10.0 and 8.5 K. The magnetic properties of the two compounds show low-dimensional characteristics because the ratio of $T_N/T(\chi_{max})$ of 0.67 and 0.85 for **1·Mn** and **4·Mn**, respectively, is significantly lower than that for a 3D antiferromagnet.[29] The field dependence of magnetization of **1·Mn** and **4·Mn** at 2 K (Figure 5, inset) shows a transition from an antiferromagnet to a spin-flop state at ca. 15 kOe, as observed for many Mn antiferromagnets.[10f,30] The magnetization is 1.54 and 1.46$N\beta$ for **1·Mn** and **4·Mn**, respectively, at 50 kOe, far from the saturation value of the Mn^{2+} ion (5$N\beta$ for $g = 2.00$), suggesting again the antiferromagnetic ordering.

To evaluate the intra- and interchain coupling, the Fisher 1D chain ($S = {}^5/_2$) model[31] based on $H = -J\sum S_i S_{i+1}$ for intrachain coupling J together with the mean field approximation[32] for interchain coupling zJ' were used to fit the magnetic data of the two compounds. The best fits were found with the parameters $J = -2.50(2)$ cm^{-1}, $g = 2.102(1)$, and $zJ' = -1.96(10)$ cm^{-1} with $R = 1.4 \times 10^{-5}$ {$R = \sum[(\chi_M T)_{obs} - (\chi_M T)_{calcd}]^2/\sum[(\chi_M T)_{obs}]^2$} for **1·Mn** and $J = -1.53(1)$ cm^{-1}, $g = 2.062(1)$, and $zJ' = -0.46(6)$ cm^{-1} with $R = 2.0 \times 10^{-5}$ for **4·Mn**. The larger zJ' of **1·Mn** indicates the stronger interchain interactions in **1·Mn** versus those in **4·Mn**. This arises from the fact that in **1·Mn** the Mn−N_3/COO chains are linked by multiple three-atom O−H···O and four-atom O−H···N_3 H-bond bridges with a short interchain Mn···Mn distance of ca. 6.5 Å, while in **4·Mn**, the interchain linkages are the NNO ligand with six diamagnetic atoms and H bonds with five diamagnetic atoms, the Mn···Mn distances being ca. 8.0 Å. Taking the multiple H-bond bridges as the main distribution to the interchain interaction, the interchain Mn···Mn coupling J' through the H-bond bridges is −0.98 cm^{-1} as $z = 2$, which is ca. 10 times greater than the interchain Mn···Mn coupling ($J' = -0.11$ cm^{-1} with $z = 4$) in **4·Mn**. It is well-known that the H bond essentially propagates antiferromagnetic interactions between metal centers[33] (even as large as −90 cm^{-1} in a Cu dimer with an O−H···O distance of 2.32 Å[34]) despite the growing number of exceptions.[35]

The main superexchange pathway presented in **1·Mn** and **4·Mn** is through the double bridges, that is, syn-syn carboxylato and EO azido bridges. Because the syn-syn carboxylate bridge provides a small metal−metal distance and results in a good overlap of the magnetic orbitals, an antiferromagnetic coupling is always induced.[36] For the EO azide bridge, theoretical studies[8b,37,38] have indicated that the main factor controlling the exchange should be the Mn−N−Mn bridging angle ϕ: a crossover between ferro- and antiferromagnetic interactions occurs at $\phi = 98°$, and the ferromagnetic interaction J increases as ϕ increases from 98°, with the maximum ferromagnetic interaction appearing at $\phi = 114°$.[38,39] In our case, the ϕ values are 121.5° for **1·Mn** and 119.8 and 119.1° for **4·Mn**, larger than the above-mentioned range of bond angles. Therefore, intrachain

(29) DeFotis, G. C.; Remy, E. D.; Scherrer, C. W. *Phys. Rev. B: Condens. Matter Mater. Phys.* **1990**, *41*, 9074.
(30) (a) Manson, J. L.; Huang, Q.-Z.; Lynn, J. W.; Koo, H.-J.; Whangbo, M.-H.; Bateman, R.; Otsuka, T.; Wada, N.; Argyriou, D. N.; Miller, J. S. *J. Am. Chem. Soc.* **2001**, *123*, 162. (b) Wang, Z.-M.; Zhang, B.; Otsuka, T.; Inoue, K.; Kobayashi, H.; Kurmoo, M. *Dalton Trans.* **2004**, 2209. (c) Salah, M. B.; Vilminot, S.; Andrÿ, G.; Richard-Plouet, M.; Bourée-Vigneron, F.; Mhiri, T.; Kurmoo, M. *Chem.—Eur. J.* **2004**, *10*, 2048.
(31) Fisher, M. E. *Am. J. Phys.* **1964**, *32*, 343.
(32) (a) Myers, B. E.; Berger, L.; Friedberg, S. A. *J. Appl. Phys.* **1969**, *40*, 1149. (b) O'Conner, C. J. *Prog. Inorg. Chem.* **1982**, *29*, 203.
(33) (a) De Munno, G.; Ventura, W.; Viau, G.; Lloret, F.; Faus, J.; Julve, M. *Inorg. Chem.* **1998**, *37*, 1458. (b) Payme, T. K.; Weyhermuller, T.; Wieghardt, K.; Chaudhuri, P. *Inorg. Chem.* **2002**, *41*, 6538 and references therein. (c) Ray, M. S.; Ghosh, A.; Chaudhuri, S.; Drew, M. G. B.; Ribas, J. *Eur. J. Inorg. Chem.* **2004**, 3110.
(34) Bertrand, J. A.; Black, T. D.; Eller, P. G.; Helm, T. N.; Mahmood, R. *Inorg. Chem.* **1976**, *15*, 2965.
(35) (a) Desplanches, C.; Ruiz, E.; Alvarez, S. *Chem. Commun.* **2002**, 2614. (b) Maspoch, D.; Catalá, L.; Gerbier, P.; Ruiz-Molina, D.; Vidal-Gancedo, J.; Wurst, K.; Roviras, C.; Veciana, J. *Chem.—Eur. J.* **2002**, *8*, 3655. (c) Tercero, J.; Diaz, C.; Ribas, J.; Mahía, J.; Maestro, M. A. *Inorg. Chem.* **2002**, *41*, 5373. (d) Tercero, J.; Diaz, C.; Ribas, J.; Ruiz, E.; Mahía, J.; Maestro, M. *Inorg. Chem.* **2002**, *41*, 6780.
(36) (a) Rodríguez-Fortea, A.; Alemany, P.; Alvarez, S.; Ruiz, E. *Chem.—Eur. J.* **2001**, *7*, 627. (b) Maji, T. K.; Sain, S.; Mostafa, G.; Lu, T.-H.; Ribas, J.; Monfort, M.; Chaudhuri, N. R. *Inorg. Chem.* **2003**, 42, 709.
(37) Villanueva, M.; Mesa, J. L.; Urtiaga, M. K.; Cortés, R.; Lezama, L.; Arriortua, M. I.; Rojo, T. *Eur. J. Inorg. Chem.* **2001**, 1581.
(38) Ruiz, E.; Cano, J.; Alvarez, S.; Alemany, P. *J. Am. Chem. Soc.* **1998**, *120*, 11122.

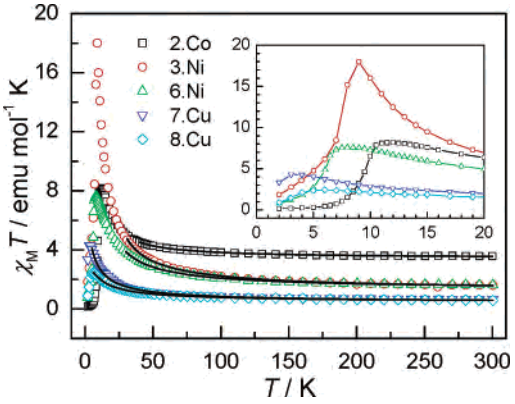

Figure 6. Plots of $\chi_M T$ vs T for **2·Co**, **3·Ni**, **7·Cu**, and **8·Cu** under an applied field of 1 kOe and **6·Ni** under an applied field of 2 kOe. The solid lines represent the theoretical fits in the high-temperature region (see text). Inset: the low-temperature region (solid lines are guides for the eye).

ferromagnetic coupling might be promoted by EO azido bridges. However, the cooperative effect of syn-syn carboxylato and EO azido bridges results in antiferromagnetic coupling between the Mn atoms, disagreeing with the above-mentioned general trend. A similar phenomenon has also been observed in $[Mn_3(N_3)_2(nta)_4(H_2O)_2]_n$ (nta = nicotinate) consisting of trinuclear subunits bridged by anti-anti carboxylato and EO azido bridges with a Mn−N−Mn angle of 118.6°.[13d] These results suggest that the carboxylato bridge might be the dominant factor in the superexchange interaction, and it seems that, except for the Mn−N−Mn angle, the coupling is also dependent on other factors such as Mn−N bond lengths, cis or trans coordination environments, or different properties of the coligands, which should influence the magnetic orbitals around the metal center.

2·Co, 3·Ni, 6·Ni, 7·Cu, and 8·Cu. These five compounds all exhibit metamagnetic behavior (Figures 6−8). At room temperature, the $\chi_M T$ values (Table 2) are all typical for the transition-metal ions involved in the compounds.[40] With the decrease of temperature, the $\chi_M T$ values increase slowly, and below 50 K, they rise up more quickly and reach a maximum at several Kelvins, and on further cooling, they decrease sharply (Figure 6). Fitting the high-temperature data to the Curie−Weiss law gives typical Curie constants, and the positive Weiss constants (Table 2) suggest the presence of dominant ferromagnetic coupling in all of these materials. Considering their structures, these results indicate that in the five compounds the intrachain interaction is ferromagnetic. Further magnetic investigation reveals that the five compounds are metamagnets. The field-cooled magnetizations under different fields are shown in Figure 7. At a low field, the χ_M versus T curves all display a maximum, suggesting the occurrence of 3D antiferromagnetic ordering in these materials. Upon increasing the field, the maximum moved to lower temperatures and became less prominent and finally disappeared at a higher applied field, indicating a metamagnetic transition. The sigmoidal shape of the M versus H plots of these materials at 2 K confirms the metamagnetic behavior (Figure 8). In the low-field region, the magnetizations increase slowly with increasing field; subsequently, they increase abruptly and finally reach saturation plateaus with the magnetizations at 50 kOe being 2.24, 2.21, 2.37, 1.12, and 1.02$N\beta$ for **2·Co**, **3·Ni**, **6·Ni**, **7·Cu**, and **8·Cu**, respec-

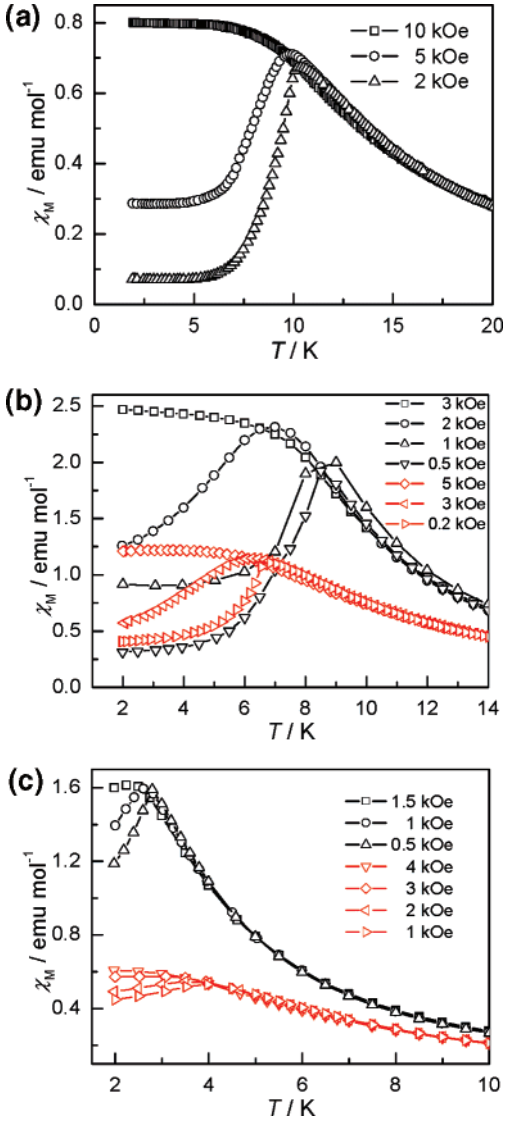

Figure 7. Plots of χ_M vs T measured on cooling under different fields for (a) **2·Co**, (b) **3·Ni** (black) and **6·Ni** (red), and (c) **7·Cu** (black) and **8·Cu** (red).

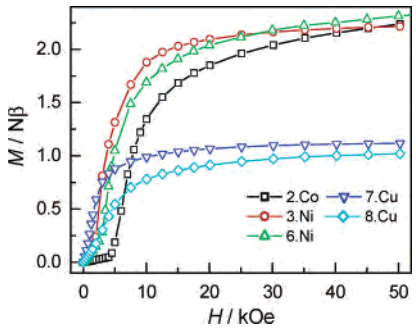

Figure 8. Plots of M vs H for **2·Co**, **3·Ni**, **7·Cu**, and **8·Cu** at 2 K and **6·Ni** at 1.8 K.

(39) (a) Karmakar, T. K.; Ghosh, B. K.; Usman, A.; Fun, H.-K.; Rivière, E.; Mallah, T.; Aromí, G.; Chandra, S. K. *Inorg. Chem.* **2005**, *44*, 2391. (b) Ni, Z.-H.; Kou, H.-Z.; Zheng, L.; Zhao, Y.-H.; Zhang, L.-F.; Wang, R.-J.; Cui, A.-L.; Sato, O. *Inorg. Chem.* **2005**, *44*, 4728.

(40) Casey, A. T.; Mitra, S. In *Theory and Application of Molecular Paramagnetism*; Mulay, L. N., Boudreaux, E. A., Eds.; John Wiley & Sons Inc.: New York, 1976.

tively, close to the expected saturated magnetization values when all spins are parallel. T_N and the critical fields can be estimated from the maximum values of $d(\chi_M T)/dT$ and dM/dH to be 9.5 K and 6.0 kOe for **2·Co**, 8.0 K and 3.0 kOe for **3·Ni**, 6.0 K and 3.5 kOe for **6·Ni**, 2.5 K and 1.0 kOe for **7·Cu**, and 3.5 K and 3.0 kOe for **8·Cu**, respectively.

On the basis of the structures of these materials, the metamagnetic behavior can be attributed to the ferromagnetic $M-N_3/COO$ chains coupled antiferromagnetically. To evaluate the couplings, magnetic models for different metal ions were used to fit the susceptibility data. For **2·Co**, the Fisher 1D chain ($S = {}^3/_2$) model was applied for the susceptibility data in the high-temperature region of 40−300 K, affording $J = 3.09(2)$ cm^{-1} and $g = 2.702(1)$ with $R = 6.4 \times 10^{-6}$. For the low-temperature region, the 1D Ising chain model ($S = {}^1/_2$)[41] was applied to fit the susceptibility between 14 and 29 K, because it is well-known that the Co^{2+} ion is most frequently Ising-like with $S_{eff} = {}^1/_2$ at low temperatures.[42] The expression $\chi = {}^1/_3\chi_{||} + {}^2/_3\chi_{\perp}$, where $\chi_{||}$ and $\chi_{\perp}$ are the parallel and perpendicular susceptibilities, respectively, was used. During the fitting, it was found that $g_{\perp}$ was almost zero, indicating the strong Ising-like anisotropy of the system, like other Co^{2+} chain complexes.[41d] Therefore, the susceptibility of the chain can be expressed as $\chi = {}^1/_3\chi_{||}$. The best fit gave $J = 7.82(6)$ cm^{-1} and $g = 10.04(2)$ with $R = 9.0 \times 10^{-5}$.

For Ni compounds, the susceptibility of the ferromagnetic chain can be calculated by eq 1

$$\chi_{chain}T = \frac{2N\beta^2g^2}{3k}\frac{AX^3 + BX^2 + CX + 1}{DX^2 + EX + 1} \qquad (1)$$

where $X = J/kT$; J is the intrachain coupling; and the coefficients are $A = 0.14709$, $B = -0.788\,967$, $C = 0.866\,426$, $D = 0.096\,573$, and $E = -0.624\,929$.[43] The best fit including the mean field approximation produced $J = 36(2)$ cm^{-1}, $zJ' = -0.8(3)$ cm^{-1}, and $g = 2.24(1)$ with $R = 1.1 \times 10^{-4}$ for **3·Ni** and $J = 26.1(7)$ cm^{-1}, $zJ' = -0.6(2)$ cm^{-1}, and $g = 2.315(7)$ with $R = 5.8 \times 10^{-5}$ for **6·Ni**. It is noted that the g values agree well with the saturation magnetizations, $2.21N\beta$ for **3·Ni** and $2.37N\beta$ for **6·Ni**, where they are equal to $gSN\beta$.

To date, a number of Ni(II) compounds containing EO azido bridging ligands have been structurally and magnetically described.[7] With two EO azido bridging ligands, the compounds generally feature a Ni−N−Ni bridging angle ϕ in a range of 100−105° and exchange J values between +13 to +73 cm^{-1}.[7,44] Density functional theory (DFT) calculations suggested that the coupling J is predicted to be ferromagnetic for all of the range of ϕ angles explored: J increases with increasing ϕ until ϕ reaches ∼104°, and then, J decreases with increasing ϕ.[38] While for the mono EO azido bridge which coexists with other bridging groups such as carboxylato-, oxo-, and polyoxometalate and pyrazolate and so forth, the magnetic nature of the complexes is no longer simply related to ϕ but is an average effect of the dissimilar bridges. For example, Meyer et al. reported a pyrazolate/EO-azide-bridged Ni(II) dimeric complex with a large ϕ value of 116.1° and a ferromagnetic intradimer coupling J of $+4.0 \pm 0.5$ cm^{-1}.[45] Mialane et al. reported a polyoxometalate (POM) containing a POM/EO-azido-bridged Ni(II) dimeric fragment, which has an unusually large ϕ value of ca. 130° while exhibiting ferromagnetic coupling between the Ni^{2+} ions with $J = 37$ cm^{-1}.[13e] All of the results affirm the assumption posed by Kahn et al.[46] for Ni(II) complexes that the EO azido group could be considered as an almost universal ferromagnetic coupler. Our case indicates that the EO azide is the dominant factor in the superexchange interaction despite the antiferromagnetic coupling promoted by the syn-syn carboxylate.

For the two Cu compounds, the expression proposed by Baker et al.[47] (eq 2) for a Heisenberg ferromagnetic $S = {}^1/_2$ chain based on the Hamiltonian $H = -J\sum S_iS_{i+1}$ was used:

$$\chi_{chain} = \frac{Ng^2\beta^2}{4kT}\left(\frac{A}{B}\right)^{2/3} \qquad (2)$$

where $A = 1.0 + 5.797\,991\,6x + 16.902\,653x^2 + 29.376\,885x^3 + 29.832\,959x^4 + 14.036\,918x^5$, $B = 1.0 + 2.797\,991\,6x + 7.008\,678x^2 + 8.653\,864\ 4x^3 + 4.574\,311\,4x^4$, and $x = J/2kT$, and the interchain interaction was estimated by the mean field model again. The best fitting for the magnetic susceptibility data resulted in $J = 80(4)$ cm^{-1}, $g = 2.13(3)$, and $zJ' = -0.17(2)$ cm^{-1} with $R = 8.0 \times 10^{-4}$ for **7·Cu** and $J = 48(1)$ cm^{-1}, $g = 2.25(1)$, and $zJ' = -0.84(2)$ cm^{-1} with $R = 2.1 \times 10^{-4}$ for **8·Cu**. The magnitude of the magnetic coupling of both Cu compounds is comparable to those of related Cu compounds.[13b,c]

In complex **7·Cu**, the copper atoms are bridged by one EO azide, one *N*-oxide group, and one carboxylate group. Exchange interaction through the pathway provided by the large axial bonding (through *N*-oxide oxygen atoms) can be expected to be less important because of the low unpaired electron density along the d_{z^2} orbital in the octahedral coordination around the copper atoms. Similarly, in **8·Cu**, the unpaired electron of each copper(II) ion clearly resides in the $d_{x^2-y^2}$ orbital, whose electron density is spread over the equatorial ligands, just including the azido and carboxylate bridges. Therefore, in both complexes, the exchange

(41) (a) Fisher, M. E. *J. Math. Phys.* **1963**, *4*, 124. (b) Miyoshi, H. *Bull. Chem. Soc. Jpn.* **1974**, *47*, 561. (c) Takeda, K.; Matsukawa, S.-I.; Haseda, T. *J. Phys. Soc. Jpn.* **1971**, *30*, 1330. (d) Sato, M.; Kon, H.; Akoh, H.; Tasaki, A.; Kabuto, C.; Silverton, J. V. *Chem. Phys.* **1976**, *16*, 405.

(42) (a) de Jongh, L. J. In *Magneto-Structural Correlations in Exchange Coupled Systems*; Willett, R. D., Gatteschi, D., Kahn, O. D., Eds.; Reidal Publishing Company: Dordrecht, Holland, 1985; pp 1−35. (b) Hatfield, W. E.; Estes, W. E.; Marsh, W. E.; Pickens, M. W.; ter Haar, L. W.; Weller, R. R. In *Extended Linear Chain Compounds*; Miller, J. S., Ed.; Plenum Press: New York, 1983; Vol. 3, pp 43−142.

(43) Monfort, M.; Resino, I.; Fallah, M. S. E.; Ribas, J.; Solans, X.; Font-Bardia, M.; Stoeckli-Evans, H. *Chem.—Eur. J.* **2001**, *7*, 280.

(44) Meyer, F.; Kozlowski, H. In *Comprehensive Coordination Chemistry II*; McCleverty, J. A., Meyer, T. J., Eds.; Pergamon: Elmsford, NY, 2004; vol. 6, pp 247−554.

(45) Leibeling, G.; Demeshko, S.; Bauer-Siebenlist, B.; Meyer, F.; Pritzkow, H. *Eur. J. Inorg. Chem.* **2004**, 2413.

(46) Aebersold, M. A.; Gillon, B.; Plantevin, O.; Pardi, L.; Kahn, O.; Bergerat, P.; von Seggern, I.; Tuczek, F.; Öhrström, L.; Grand, A.; Lelièvre-Berna, E. *J. Am. Chem. Soc.* **1998**, *120*, 5238.

(47) Baker, G. A.; Rushbrooke, G. S. *Phys. Rev.* **1964**, *135*, 1272.

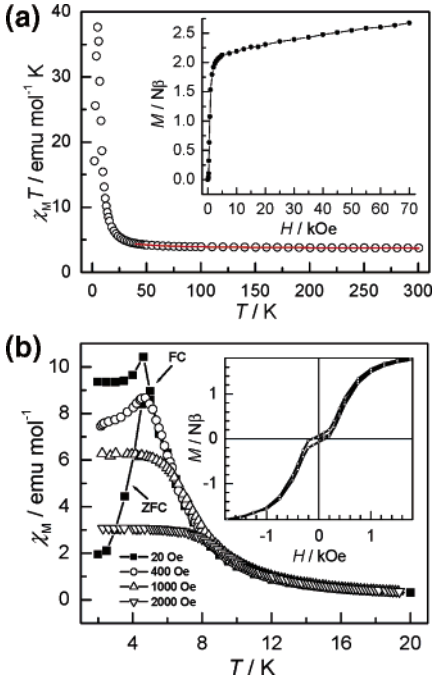

Figure 9. Magnetism for **5·Co**. (a) Plot of $\chi_M T$ vs T. Red solid line represents the best theoretical fit. Inset: plot of M vs H at 1.8 K; (b) the zero-field-cooled (ZFC) magnetization and field-cooled magnetization (FC) at 20 Oe (highlighted by filled squares) and FC under different fields. Inset: hysteresis in low field at 2.0 K.

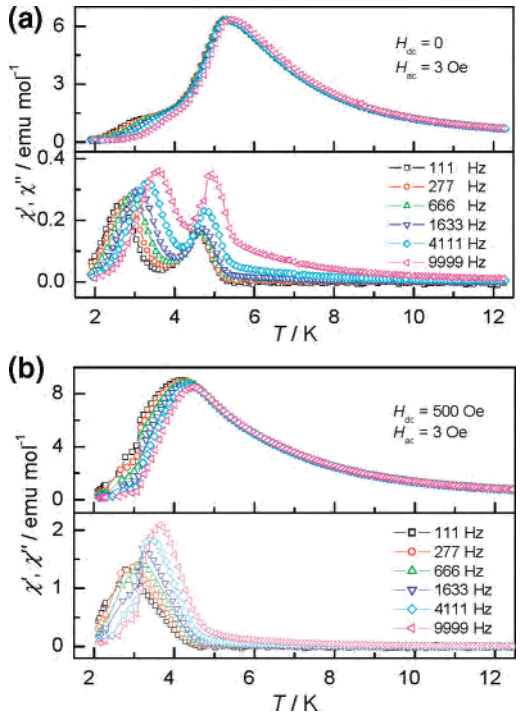

Figure 10. AC susceptibilities for **5·Co**: temperature dependence of AC susceptibilities in (a) a zero DC field and (b) a 500 Oe DC field with an oscillating field of 3 Oe.

interactions along the chains would be expected to depend predominantly on the EO azide and the syn-syn carboxylate bridges. For the syn-syn carboxylato bridge, it is expected to promote antiferromagnetic coupling. For the EO azido bridge in the basal−basal disposition, it has been widely cited that it favors antiferromagnetic interactions when the Cu−N−Cu angle is larger than 108°.[15b,26b] From the DFT study by Ruiz et al., the Cu−N cutoff distance for ferromagnetic interactions is 2.05 Å.[38] In the case of **7·Cu**, the Cu−N−Cu bridging angle of 106.6°, lower than 108°, and a Cu−N distance of 1.959 Å, shorter than 2.05 Å, could give rise to ferromagnetic coupling. In this way, the actual ferromagnetic coupling in **7·Cu** suggests that the EO azido bridge is a more efficient magnetic pathway than the syn-syn carboxylato bridge. However, it appears that the ferromagnetic coupling in **8·Cu**, containing a syn-syn carboxylato bridge and an EO azido bridge with a Cu−N−Cu angle of 124.3° and Cu−N distances of 1.986 and 1.998 Å, disagrees with the above trends. This situation may be ascribed to the countercomplementarity effect proposed by Thompson et al. and Escuer et al. using molecular orbital calculations: the antiferromagnetic contributions of each bridge (i.e., the syn-syn carboxylato bridge and the EO azido bridge) almost cancel each other out, and the ferromagnetic term dominates.[13b,c]

It should be noted that the difference in J values of **7·Cu** and **8·Cu** reflects subtle geometric differences of Cu^{2+} ions between the two compounds. In **7·Cu**, the Cu^{2+} ion resides in an elongated octahedron, and the dihedral angle between the equatorial planes of two adjacent Cu^{2+} ions is 66°. In contrast, in **8·Cu**, the Cu^{2+} ion exhibits a distorted square-pyramidal geometry with trigonal bipyramidal character, the distortion parameter τ being 0.22, and the dihedral angle between the two basal planes is 34.7°. The greater distortion and smaller dihedral angle, in particular, the even larger Cu−N−Cu angle of **8·Cu**, remove the orthorgonality between the magnetic orbitals of Cu^{2+} ions and reduce the ferromagnetic contribution, which still dominates the total exchange. The larger zJ' value of **8·Cu** versus that of **7·Cu** agrees with the closer interchain Cu···Cu separations in the structure and the higher critical field for the antiferromagnetic−ferromagnetic transition of **8·Cu** versus that of **7·Cu**.

5·Co. The DC magnetic investigations of **5·Co** (Figure 9, Table 2) revealed that it shows metamagnetic behavior as did the five compounds discussed above, with a lower critical field of 400 Oe. Fitting the susceptibility data above 40 K to the Fisher 1D chain ($S = {}^3/_2$) model[31] led to $J = 2.06(2)$ cm^{-1} and $g = 2.785(2)$ with $R = 1.1 \times 10^{-4}$. The low-temperature susceptibility (8−40 K) was simulated by the 1D Ising chain model[41,42] ($S = {}^1/_2$), including the mean field approximation; the best fit gave $J = 12.6(2)$ cm^{-1}, $zJ' = -0.5(1)$ cm^{-1}, and $g = 9.10(9)$ with $R = 5.3 \times 10^{-5}$.

However, the field-cooled magnetization and zero-field-cooled magnetization data at a low field of 20 Oe showed the irreversibility below ca. 5 K (Figure 9b, highlighted), and a small hysteresis with a coercive field of 100 Oe was observed at 2.0 K (Figure 9b, inset). This might indicate the nonlinear character of the antiferromagnetic interaction between ferromagnetic chains. To further understand the magnetism of **5·Co**, measurements on specific heat (C_P) and AC susceptibility were performed. The magnetic contribution, C_m, was obtained by the C_P data subtracted by an estimated lattice contribution based on the Debye T^3 law. Under a zero field, the C_m/T data show a sharp peak at 5.1 K, indicating the magnetic transition or long-range ordering

at this temperature (Figure S6, Supporting Information). Above the temperature, there is a broad hump probably featuring the short-range order of the Ising-like $Co-N_3/COO$ chain.[48] The AC data reveal more features of the magnetism of **5·Co** in the low-temperature range (Figure 10; Figures S7 and S8, Supporting Information). The AC susceptibilities, obtained by a 3 Oe AC field oscillating at 111−9999 Hz under 0 and 500 Oe DC fields are respectively shown in Figure 10a and b. At zero DC field, the in-phase part, χ', of all of the frequencies rises smoothly below 12 K and exhibits a frequency-independent maximum value at 5.3 K, which may be assigned to the antiferromagnetic transition, as revealed by C_P measurement. Below the maximum, the χ' curve has a weak plateau around 3 K which is sensitive to frequency; that is, the peak temperature increases and the peak height decreases with increasing frequency. The out-of-phase part, χ'', also supports the above observations. At the antiferromagnetic transition temperature of ca. 5 K, the χ'' curve shows a peak with a weak frequency dependence, followed by a second peak at $T \sim 3$ K which is strongly frequency-dependent and even more significant than the peak at ca. 5 K. The magnetic relaxation of χ'' obeys the Arrhenius law, $\tau = \tau_0 \exp(E_a/k_BT)$, and the best fit gave $\tau_0 = 5.1 \times 10^{-11}$ s and $E_a/k_B = 45$ K (Figure S7, Supporting Information). Considering the system of weakly coupled ferromagnetic chains, this magnetic relaxation might arise from the finite size effect of the weakly coupled ferromagnetic chain as a result of the defect.[49] When applying a DC field of 500 Oe, which is higher than the metamagnetic critical field, the χ'' component shows one frequency-dependent peak at ca. 3 K, and the peak at ca. 5 K seems to be suppressed; the relaxation time follows the Arrhenius law with $\tau_0 = 2.8 \times 10^{-12}$ s and $E_a/k_B = 57$ K. Such behavior is similar to those observed in some cobalt chain compounds.[50] In C_m/T data, the sharp peak became less significant (Figure S6, Supporting Information) when an external field was applied, and this confirmed the above result from AC measurements. Finally, the isothermally frequency-dependent AC susceptibilities at 2.63 K (Figure S8, Supporting Information) show a gradual decrease in χ' and a broader maximum in χ'' with respect to frequency. The locus or Cole−Cole plot of χ'' versus χ' could not be fitted successfully by the generalized Debye model.[51] This indicates that the observed relaxation process is probably not a single one, and it deserves further study.

Conclusions

With two isomers of pyridine carboxylate *N*-oxide, NNO and INO, of different coordination geometries being involved in metal−azido systems, seven 2D Mn(II), Co(II), Ni(II), and Cu(II) coordination polymers and one 3D Cu(II) coordination polymer have been synthesized and characterized structurally and magnetically. All complexes are made up of mono EO azido and mono syn-syn carboxylato spontaneously bridged $M-N_3/COO$ chains that were rarely observed before. The chains are further connected by the organic ligands to form the 2D layers for **1·Mn**, **2·Co**, **3·Ni**, **4·Mn**, **5·Co**, **6·Ni**, and **8·Cu** and the 3D framework for **7·Cu**. The two Mn(II) complexes (**1·Mn** and **4·Mn**) are antiferromagnets, whereas the Ni(II) and Cu(II) complexes (**3·Ni** and **6·Ni**, **7·Cu** and **8·Cu**) and one Co(II) complex (**2·Co**) exhibit metamagnetic behaviors. **5·Co** is also a metamagnet but exhibits magnetic relaxation. This work demonstrates that the combination of short ligands like azido and coligands of long spacers can result in such materials with lower dimensional magnetism. The coligand in the metal−azido system can be used to tune the structure and the magnetic interaction of the $M-N_3$ motif, the connection between the motifs, and the interchain or interlayer magnetic interactions. It may be expected that the interchain interaction will be further weakened if longer ligands are employed, thus leading to SCM.

Acknowledgment. We thank Prof. Mohamedally Kurmoo of Université Louis Pasteur for valuable discussions, Dr. Haoling Sun for his kind help with magnetic measurements, and Prof. Shao-Kui Su and Li Lu of the Institute of Physics, Chinese Academy of Sciences, for their kind help in the measurement of heat capacity. Financial support from NSFC (20571005, 20221101, 20490213, and 20423005), MOST of China (2006CB601100), and the Founder Foundation of PKU are gratefully acknowledged.

Supporting Information Available: X-ray crystallographic files in CIF format for the structures in this work, a PDF file containing Figures S1−S8 and Tables S1−S4. This material is available free of charge via the Internet at http://pubs.acs.org.

IC060225W

(48) Carlin, R. L. *Magnetochemistry*; Springer-Verlag: Berlin, 1986; p 165.
(49) (a) Coulon, C.; Clérac, R.; Lecren, L.; Wernsdorfer, W.; Miyasaka, H. *Phys. Rev. B: Condens. Matter Mater. Phys.* **2004**, *69*, 132408. (b) Bogani, L.; Caneschi, A.; Fedi, M.; Gatteschi, D.; Massi, M.; Novak, M. A.; Pini, M. G.; Rettori, A.; Sessoli, R. Vindigni, A. *Phys. Rev. Lett.* **2004**, *92*, 207204. (c) Bogani, L.; Sessoli, R.; Pini, M. G.; Rettori, A.; Novak, M. A.; Rosa, P.; Massi, M.; Fedi, M. E.; Giuntini, L.; Caneschi, A.; Gatteschi, D. *Phys. Rev. B: Condens. Matter Mater. Phys.* **2005**, *72*, 064406.
(50) (a) Toma, L. M.; Lescouëzec, R.; Lloret, F.; Julve, M.; Vaissermann, J.; Verdaguer, M. *Chem. Commun.* **2003**, 1850. (b) Li, X.-J.; Wang, X.-Y.; Gao, S.; Cao, R. *Inorg. Chem.* **2006**, *45*, 1508. (c) Kumagai, H.; Kepert, C. J.; Kurmoo, M. *Inorg. Chem.* **2002**, *41*, 3410.
(51) (a) Miyasaka, H.; Clérac, R.; Mizushima, K.; Sugiura, K.-i.; Yamashita, M.; Wernsdorfer, W.; Coulon, C. *Inorg. Chem.* **2003**, *42*, 8203. (b) Aubin, S. M. J.; Sun, Z.; Pardi, L.; Krzystek, J.; Folting, K.; Brunel, L.-C.; Rheingold, A. L.; Christou, G.; Hendrickson, D. N. *Inorg. Chem.* **1999**, *38*, 5329. (c) Cole, K.; Cole, R. H. *J. Chem. Phys.* **1941**, *9*, 341.